Infrared Physics & Technology 59 (2013) 36–40

Contents lists available at SciVerse ScienceDirect

Infrared Physics & Technology

journal homepage: www.elsevier.com/locate/infrared

Electronic and optical properties of 4.2 μm"N" structured superlattice MWIR photodetectors

O. Salihoglu [a], M. Hostut [b], T. Tansel [c], K. Kutluer [c], A. Kilic [e], M. Alyoruk [d], C. Sevik [e], R. Turan [c], Y. Ergun [e,*], A. Aydinli [a]

[a] Bilkent University, Dept. of Physics, Ankara, Turkey
[b] Akdeniz University, Faculty of Education, Antalya, Turkey
[c] Middle East Technical University, Dept. of Physics, Ankara, Turkey
[d] Dumlupinar University, Dept. of Physics, Kutahya, Turkey
[e] Anadolu University, Dept. of Physics, Eskisehir, Turkey

ARTICLE INFO

Article history:
Available online 5 January 2013

Keywords:
Superlattice
Barrier design
N structure
MWIR photodetector
Infrared detector
SiO_2 passivation

ABSTRACT

We report on the development of a new structure for type II superlattice photodiodes that we call the "N" design. In this new design, we insert an electron barrier between InAs and GaSb in the growth direction. The barrier pushes the electron and hole wavefunctions towards the layer edges and under bias, increases the overlap integral by about 25% leading to higher detectivity. InAs/AlSb/GaSb superlattices were studied with density functional theory. Both AlAs and InSb interfaces were taken into account by calculating the heavy hole–light hole (HH–LH) splittings. Experiments were carried out on single pixel photodiodes by measuring electrical and optical performance. With cut-off wavelength of 4.2 μm at 120 K, temperature dependent dark current and detectivity measurements show that the dark current is 2.5×10^{-9} A under zero bias with corresponding R_0A resistance of $1.5 \times 10^4\ \Omega\,cm^2$ for the $500 \times 500\ \mu m^2$ single pixel square photodetectors. Photodetector reaches BLIP condition at 125 K with the BLIP detectivity (D^*_{BLIP}) of 2.6×10^{10} Jones under 300 K background and −0.3 V bias voltage.

1. Introduction

Recently, type-II superlattice (T2SL) infrared photodetectors have received great attention for civilian, military and medical applications. Furthermore, T2SL system is becoming an alternative technology for mercury cadmium telluride (MCT) and QWIP technologies. Ability to control the band gap by varying the InAs thickness [1], with suppressed Auger recombination rates [2], reduced interband tunneling due to higher effective masses of electrons and holes [3] makes T2SL a very promising technology for most of the infrared region (3–30 μm). In the quest of achieving state of art infrared photodetectors, further improvements such as, reducing the dark current level due to generation recombination (*G–R*) mechanisms and surface conductive channels, are needed. Furthermore, most of the photodetectors in the market requires low operating temperatures that is inconvenient for many applications. Ability to operate higher operating temperatures (HOTs) will reduce cost, volume, weight and power requirements.

Introducing a barrier inside the superlattice period is an efficient way to solve listed problems above. Many such barriers with intuitive material designs have been proposed such as, nBn design [4], PbIbN design [5], CBIRD structure [6] and M structure design [7]. These designs aim to block one type of carrier while allowing other type of carriers. These designs have been very effective with the ability to drastically reduce the dark current and increase the BLIP temperature above 100 K. In InAs/GaSb SL p–i–n photodiodes, taking the advantage of the close lattice constants, Nguyen et.al. inserted asymmetric AlSb barrier layer inside the GaSb layer and calling it the "M" structure. M structure blocks the thermal electrons to reduce dark current. Further, it also increases detectivity by increasing electron–hole wavefunctions overlap integral due to the AlSb barrier pushing the electron and hole wave functions towards the layer edges.

In this report, we introduce a new structure design that we call as "N" design. In this material design, we insert an AlSb layer between the InAs and GaSb layer in the growth direction. This design works similar to M design but it allows better electron–hole wavefunction overlap under reverse bias conditions, leading to efficient optical absorption. We expect that the N design delivers better optical performance and similar electrical performance when compared with the M design. However, due to relatively large constant mismatch between InAs (6.0584 Å) and AlSb (6.1355 Å) unlike AlSb on GaSb (6.0959 Å) unwanted trap states may be generated at the

* Corresponding author.
E-mail address: yergun@anadolu.edu.tr (Y. Ergun).

1350-4495/$ - see front matter © 2012 Elsevier B.V. All rights reserved.
http://dx.doi.org/10.1016/j.infrared.2012.12.007

interface. This may be overcome with AlSb layers thinner than the critical thickness. Spitzer et al. showed that InSb like interfaces in AlSb/InAsSb superlattices grow perfectly pseudomorphically while AlAs like interfaces relax [8]. As will be shown, our dark current measurements show that lattice mismatch does not affect device performance, dramatically.

2. Theory/calculation

Density functional theory (DFT) calculations were performed using the plane wave basis pseudopotential method as implemented in the ABINIT code [9]. The simulations were carried out using the Fritz-Haber Institute (FHI) type pseudopotentials, in which the exchange–correlation energy is evaluated in the local density approximation (LDA), using Perdew–Wang parametrization [10] of Ceperley–Alder electron-gas data [11]. For all structures, the plane-wave energy cutoff of 30 Ha were found to be enough for convergence of all the reported quantities.

In particular we have performed systematical calculations for several N-structure InAs/AlSb/GaSb based T2SL structures in order to clear out the effect of AlSb blocking barrier and layer thicknesses on the band gap and HH–LH splitting energies, which are particularly important in the suppression of non-radiative electron–hole recombination in practical detector applications. Due to the well-known tendency of the DFT in order to underestimate the band gap values of semiconductors and insulators, we tested different types of pseudopotentials and proceeded to handle the investigation with the one gives the largest band gap energy for the InAs6/AlSb2/GaSb4 structure. Eventually, the selected pseudopotentials give 0.001, 1.110, and 0.480 eV for the band gap values of bulk InAs, AlSb and GaSb, respectively (Experimentally predicted band gap values are 0.43, 1.65, and 0.81 eV [12] for bulk InAs, AlSb and GaSb, respectively.). In this study, to calculate the exact band gap values, advanced methods such as GW approximation [13] has not been applied because the computational cost would be extreme for the super lattice structures having such a large super cell.

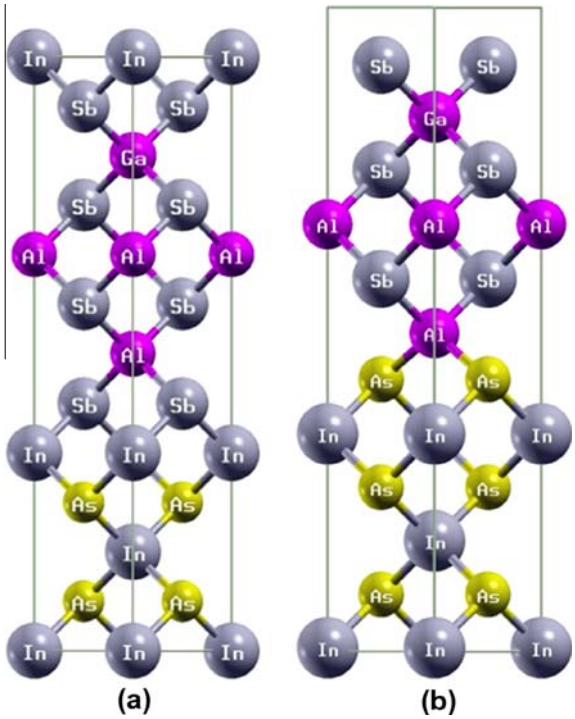

Fig. 1. (InAs)3/(AlSb)2/(GaSb)1 structures with (a) InSb and (b) AlAs interfaces.

While constructing InAs/AlSb/GaSb structures of two different transition interfaces, InSb and AlAs, they can be formed between the InAs and AlSb layers, see Fig. 1a and b. The effect of these two transition structures on HH–LH splitting energies is examined by band structure calculations of the InAsn/AlSb2/GaSbn-2 (n = 2–8) superlattices with both InSbAl and InAsAl interfaces. Calculated band structures of the InAs3/AlSb2/GaSb1 superlattices are depicted in Fig. 2a and b as illustrations. In Fig. 3, we show the effect of these transition interface types on the HH–LH splittings of superlatticeswith different number of layers, n.

If the transition interface is InSb, energy difference of HH–LH splitting shows ascending behavior while if it is AlAs, HH–LH splitting shows descending range with the increasing layer numbers of the superlattice structures. Range of variations are about 50 meV

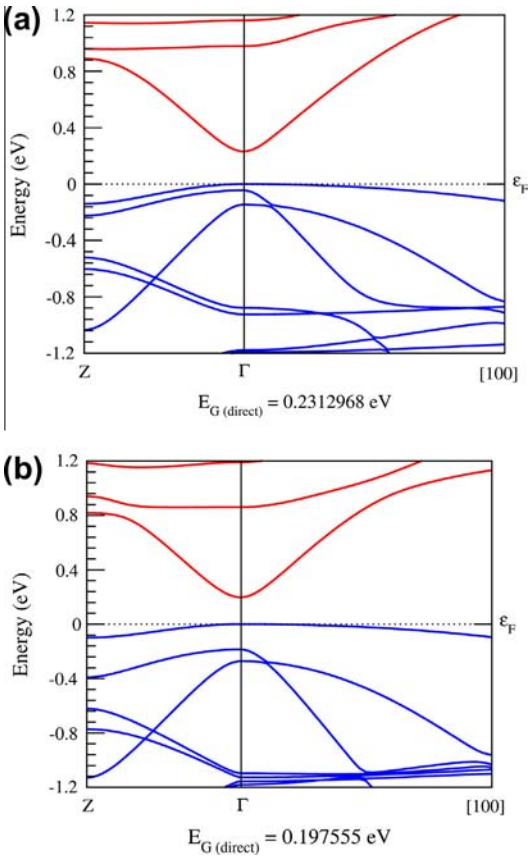

Fig. 2. Band structure of (InAs)3/(AlSb)2/(GaSb)1 structures with (a) InSb and (b) AlAs interfaces.

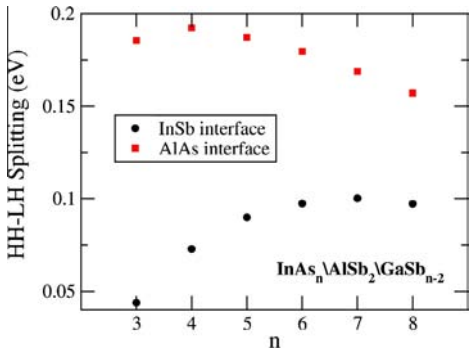

Fig. 3. Heavy hole–light hole splittings of InAs/AlSb/GaSb structures with increasing layer thicknesses.

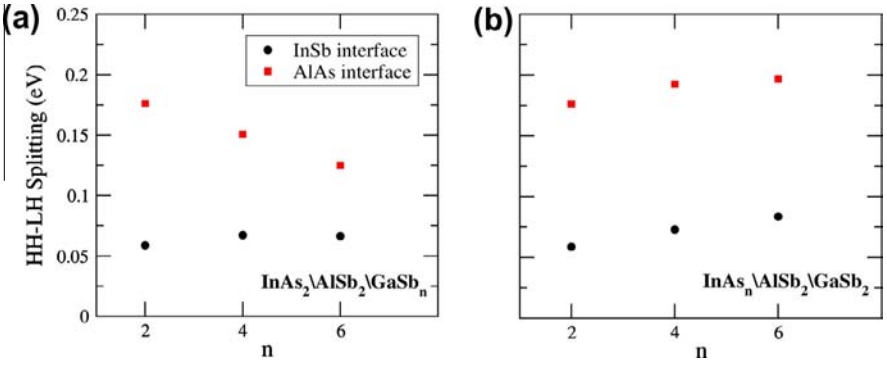

Fig. 4. HH–LH splittings of the InAs/AlSb/GaSb structures as a function of (a) GaSb and (b) InAs layer thicknesses.

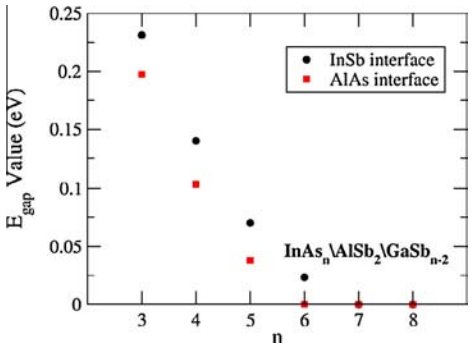

Fig. 5. E_{gap} values for InAs/AlSb/GaSb superlattices.

and the splitting energies of the structures with AlAs interfaces are higher than the InSb ones.

In Fig. 4, we show the effects of layer thickness of InAs and GaSb regions with two different transition interfaces. Structures with the InSb interfaces show increasing splitting value while AlAs interfaced structures show decreasing splitting value with the increase in the number of GaSb layers, see Fig. 4a. However, for both types of interfaces, the splitting values increase with the increasing number of InAs layer thickness, see Fig. 4b.

Fig. 5 shows the calculated E_{gap} values of superlattices as a function of number of layers (n). The E_{gap} values show descending range with both interfaces and there is no significant difference between these two structures when the well-known discrepancy of the LDA type pseudopotentials on band gap of semiconductors and insulators is considered. On the other hand, the calculated band gap values for $n > 6$ show that the used pseudopotential is not accurate enough in order to predict the semiconductor nature of these super lattice structures.

Fig. 6 shows the effect of the GaSb and InAs layer thicknesses on the E_{gap} values of the superlattice structures. Our results exhibit that electronic band gap values show minor deviations with the type of transition interfaces. However, increment in the number of InAs layers leads to considerable difference in the E_{gap} values on the contrary to the increment in GaSb layers.

3. Materials and methods

Fig. 7a shows a schematic draw of the N structure energy band diagram. An AlSb layer inserted between InAs and GaSb layers which blocks the thermal electrons. Structure gives the impression of the Latin capital letter N, which lead us to call this new design as N structure design. Fig. 7b shows layer makeup of the actual superlattice structure. It starts with 100 nm thick GaSb buffer layer and 20 nm $Al_{(x)}GaAs_{(y)}Sb$ as an insulator and etch stop layer, followed by 1000 nm GaSb:Be ($p = 1.0 \times 10^{17}$ cm^{-3}) p contact layer. p–i–n part of the design consist of 90 periods 9 monolayers (MLs) of InAs/2 MLs of AlSb/8.5 MLs of GaSb:Be ($p = 1.5 \times 10^{17}$ cm^{-3}) p-type layers, 60 periods 9 MLs of InAs/2 MLs of AlSb/8.5 MLs of GaSb i-layers, 40 periods 9 MLs of InAs:Te (n: 5×10^{17} cm^{-3})/2 MLs of AlSb/8.5 MLs of GaSb n-type layers and structure is terminated by 20 nm InAs:Te (n: 5×10^{17} cm^{-3}) cap layer to assure good ohmic contact. The sample studied in this work was grown commercially (IQE Inc. USA) with molecular beam epitaxy on a GaSb substrate.

Single pixel photodetectors were fabricated with mesa sizes ranging from 100×100 to 700×700 μm^2. To minimize surface damage, mesas have been fabricated by standard lithography and phosphoric acid based wet etch solution. The etch process has been stopped when etch depth reached the bottom contact layer. The complete fabrication processes can be found elsewhere [14]. A protective 250 nm thick SiO_2 layer has been deposited using plasma

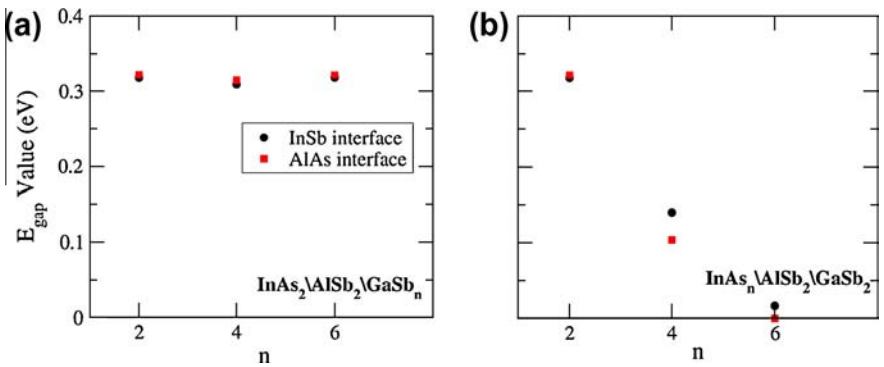

Fig. 6. E_{gap} values of the InAs/AlSb/GaSb structures as a function of (a) GaSb and (b) InAs layer thicknesses.

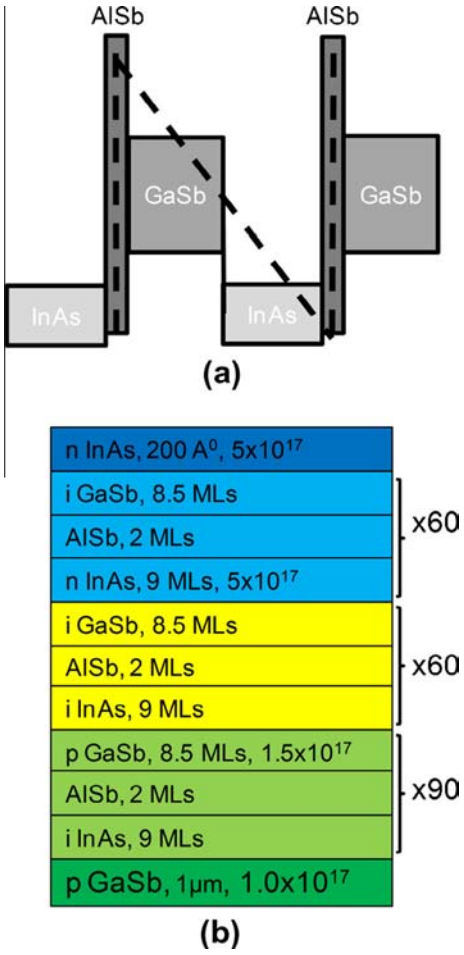

Fig. 7. (a) "N" structure superlattice and (b) p–i–n superlattice photodiode structure.

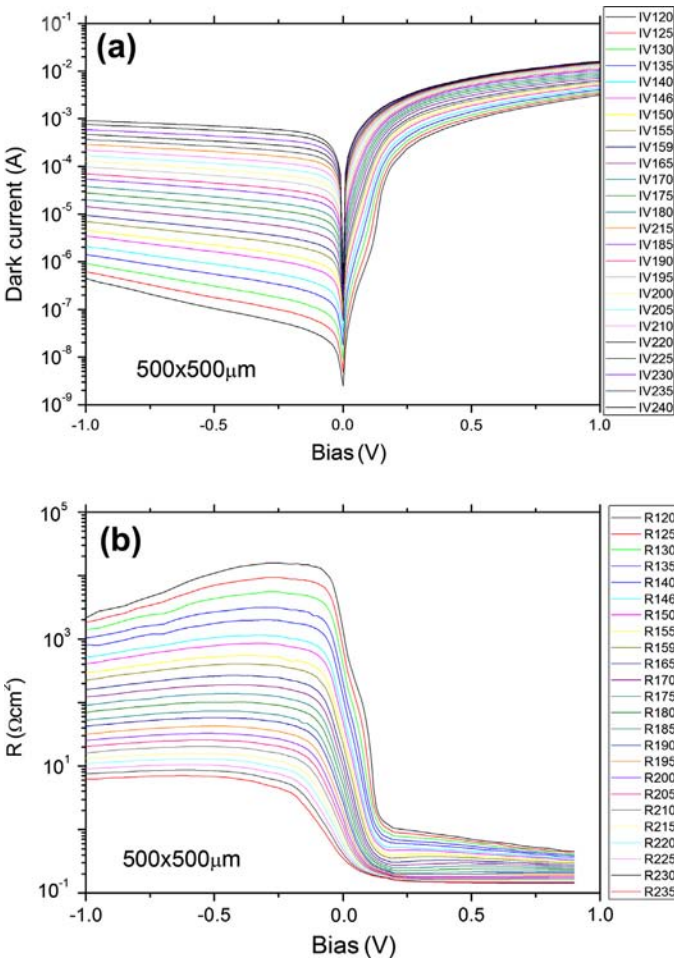

Fig. 8. (a) Dark current measurement for different temperatures. (b) Dynamic resistance measurements for different temperatures.

enhanced chemical vapor deposition (PECVD) system at 160 °C with 2%SiH_4/N_2 and N_2O gas flows of 180 sccm and 225 sccm, respectively. Ohmic contacts were made by evaporating 5 nm Titanium (Ti) and 200 nm Gold (Au) on the bottom and top contact layers of the detectors. Sample was bonded to a chip carrier for further characterization.

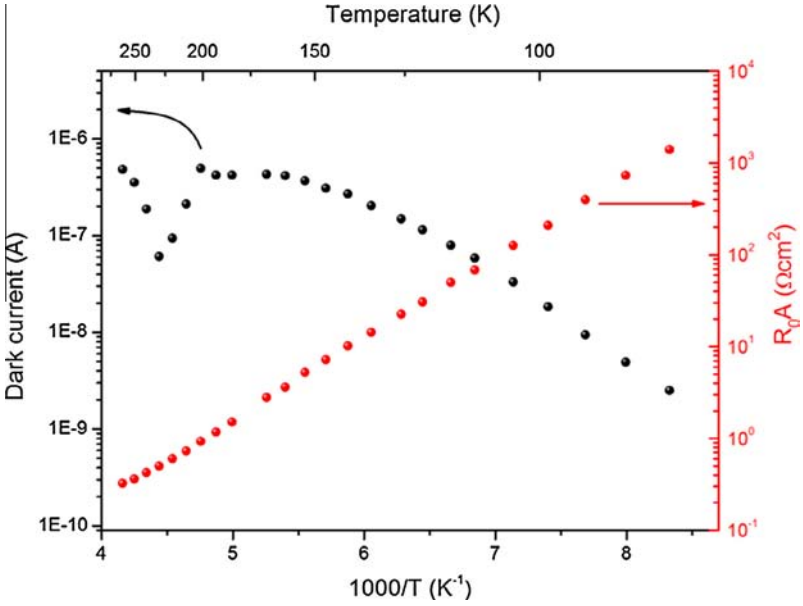

Fig. 9. Dark current and dynamic resistance vs.1000/*T* graph.

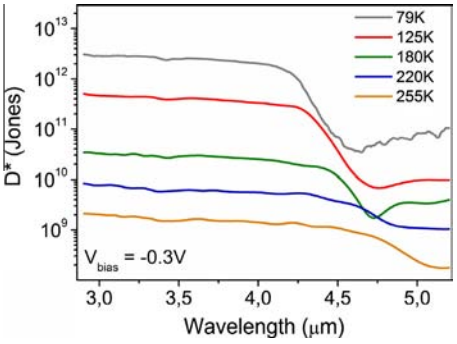

Fig. 10. Photoresponsivity vs. wavelength graph for the operating temperatures between 79 K and 250 K. Under −0.3 V bias.

4. Results

Dark current density measurement for $500 \times 500\ \mu m^2$ square single pixel photodetector for different temperatures between 120 K and 240 K has been realized (Fig. 8a), corresponding dynamic resistance vs. applied bias graph is shown in Fig. 8b. At 120 K, results shows 1.5×10^{-9} A dark current and $1.5 \times 10^4\ \Omega\,cm^2$ dynamic resistance which is very promising towards HOT application.

Fig. 9 shows dark current density and dynamic resistance area product vs. 1000/T graph for $500 \times 500\ \mu m^2$ photodiode for different temperatures under zero bias. The I–V curve shows the effects of the diffusion current for temperatures higher than 120 K. For higher temperatures, Arrhenius behavior has been observed.

Spectral response of the photodetectors has been measured using calibrated blackbody source at 450 °C (Newport, Oriel 67000), lock-in amplifier (SRS, SR830 DSP) and mechanical chopper (SRS, SR540) system. Details of the measurement can be found elsewhere [15]. For single pass front illumination condition, highest quantum efficiency (QE) of the photodetector has been determined as 15% around wavelength of 3.5 μm. Quantum efficiency is directly related with the thickness of the absorbing region and can be increased with thicker absorbing region. The cut-off wavelength of the device is determined to be 4.2 μm at 77 K. Additionally, Fig. 10 shows photoresponsivity vs. wavelength graph for the operating temperatures between 79 K and 250 K. Under −0.3 V bias, the peak D^* was equal to 2.9×10^{12} Jones for the photodetector at 4.0 μm and 77 K. BLIP temperature has been determined as 125 K for the N design barrier structure.

5. Conclusions

In conclusion, we introduce a new N design structure with very low dark current and high dynamic resistance at 120 K. N designed superlattice photodetectors show dark current as low as 2.5×10^{-9} A at 120 K and under zero applied bias. Corresponding resistance area product was $1.5 \times 10^4\ \Omega\,cm^2$ for the $500 \times 500\ \mu m^2$ single pixel square photodetectors. Quantum efficiency (QE) of the photodetector has been determined as 15% for single pass front illumination condition. Quantum efficiency can be further increased with thicker absorber regions and multipass designs. Temperature dependent dark current measurements revealed Arrhenius behavior with bulk diffusion current effective for the temperatures higher than 120 K. Since AlSb is only two monolayers thick, it does not seem to be generating large amount of electrically active interface states. Our results show that this lattice mismatch is not large enough to reduce device performance significantly. Photodetector reaches BLIP condition at 125 K with the BLIP detectivity (D^*_{BLIP}) of 2.6×10^{10} Jones under 300 K background and −0.3 V bias voltage.

Acknowledgments

C. Sevik acknowledges the support from The Scientific and Technological Research Council of Turkey (TUBITAK), M. Hostut and Y. Ergun acknowledge the support of Akdeniz University and Anadolu University (BAP Grants: 2012.01.0110.002 and 1104F073-1104F074), respectively.

References

[1] J. Wei, M. Razeghi, Modeling of type-II InAs/GaSb superlattices using an empirical tight-binding method and interface engineering, Phys. Rev. B 69 (2004) 085316.
[2] C.H. Grein, P.M. Young, H. Ehrenreich, Minority-carrier lifetimes in ideal Ingasb/Inas superlattices, Appl. Phys. Lett. 61 (1992) 2905–2907.
[3] D.L. Smith, C. Mailhiot, Proposal for strained type-I*i* superlattice infrared detectors, J. Appl. Phys. 62 (1987) 2545–2548.
[4] J.B. Rodriguez, E. Plis, G. Bishop, et al., NBn structure based on InAs/GaSb type-II strained layer superlattices, Appl. Phys. Lett. 91 (2007) 043514.
[5] N. Gautam, H.S. Kim, M.N. Kutty, et al., Performance improvement of longwave infrared photodetector based on type-II InAs/GaSb superlattices using unipolar current blocking layers, Appl. Phys. Lett. 96 (2010) 231107.
[6] D.Z.Y. Ting, C.J. Hill, A. Soibel, et al., A high-performance long wavelength superlattice complementary barrier infrared detector, Appl. Phys. Lett. 95 (2) (2009).
[7] B.M. Nguyen, D. Hoffman, P.Y. Delaunay, et al., Dark current suppression in type II InAs/GaSb superlattice long wavelength infrared photodiodes with M-structure barrier, Appl. Phys. Lett. 91 (2007) 163511.
[8] R. Spitzer et al., Quality of AlAs-like and InSb-like interfaces in InAs/AlSnsuperlattices: an optical study, Appl. Phys. Lett. 62 (1993) 2274.
[9] X. Gonze, B. Amadon, et al., Computer Phys. Commun. 180 (2009) 2582.
[10] J.P. Perdew, Y. Wang, Phys. Rev. B 45 (1992) 13244.
[11] D.M. Ceperley, Phys. Rev. Lett. 45 (1980) 566.
[12] C. Kittel, Introduction to Solid State Physics, seventh ed., Wiley, 1996. p. 201.
[13] X. Gonze, G.-M. Rignanese, et al., A brief introduction to the ABINIT software package, Zeit. Kristallogr. 220 (2005) 558–562.
[14] O. Salihoglu, A. Muti, K. Kutluer, et al., Atomic layer deposited Al_2O_3 passivation of type-II InAs/GaSb superlattice photodetectors, J. Appl. Phys. 111 (2012) 074509.
[15] T. Tansel, K. Kutluer, O. Salihoglu, et al., Effect of the passivation layer on the noise characteristics of mid-wave infrared InAs/GaSb superlattice photodiodes, Photon. Technol. Lett., IEEE 24 (2012) 9.